American Mineralogist, Volume 101, pages 2539–2543, 2016

Yangite, $PbMnSi_3O_8 \cdot H_2O$, a new mineral species with double wollastonite silicate chains, from the Kombat mine, Namibia

ROBERT T. DOWNS[1], WILLIAM W. PINCH[2], RICHARD M. THOMPSON[3,*], STANLEY H. EVANS[1], AND LAUREN MEGAW[1]

[1]Department of Geosciences, University of Arizona, 1040 East 4th Street, Tucson, Arizona 85721, U.S.A.
[2]19 Stonebridge Lane, Pittsford, New York 14534, U.S.A.
[3]School of Information, University of Arizona, 1103 East 2nd Street, Tucson, Arizona 85721, U.S.A.

ABSTRACT

A new chain-silicate mineral species, yangite, ideally $PbMnSi_3O_8 \cdot H_2O$, has been found on a specimen from the Kombat mine, Otavi Valley, Namibia. Associated minerals are melanotekite and rhodochrosite. Yangite is colorless to pale brown in transmitted light, transparent with white streak and vitreous luster. Broken pieces of yangite crystals are bladed or platy, and elongated along [010]. It is sectile with a Mohs hardness of ~5; cleavage is perfect on {101} and no twinning or parting was observed. The measured and calculated densities are 4.14(3) and 4.16 g/cm^3, respectively. Optically, yangite is biaxial (–), with n_α = 1.690(1), n_β = 1.699(1), n_γ = 1.705(1), Y = b, $Z \wedge c$ = 11°, and $2V_{meas}$ = 77(2)°. It is insoluble in water, acetone, and hydrochloric acid. An electron microprobe analysis demonstrated that the sample was relatively pure, yielding the empirical formula (with calculated H_2O) $Pb_{1.00}Mn^{2+}_{1.00}Si_{3.00}O_8 \cdot H_2O$. Yangite is triclinic and exhibits space group symmetry $P\bar{1}$ with unit-cell parameters a = 9.6015(9), b = 7.2712(7), c = 7.9833(8) Å, α = 105.910(4), β = 118.229(4), γ = 109.935(5)°, and V = 392.69(7) Å^3. Its crystal structure is based on a skeleton of double wollastonite SiO_4 tetrahedral chains oriented parallel to [010] and interlinked with ribbons of Mn- and Pb-polyhedra. Yangite represents the first chain silicate with two-connected double chains and possesses all of the structural features of a hypothetical triclinic $Ca_2Si_3O_8 \cdot 2H_2O$ phase proposed by Merlino and Bonaccorsi (2008) as a derivative of the okenite structure. The difference in the H_2O component between the hypothetical phase and yangite likely is a consequence of the larger Pb^{2+} with its lone-pair electrons in yangite replacing the smaller Ca^{2+} in the hypothetical phase.

Keywords: Yangite, chain silicate, wollastonite chains, crystal structure, X-ray diffraction, Raman spectra

INTRODUCTION

A new mineral species and new type of chain silicate, ideal formula $PbMnSi_3O_8 \cdot H_2O$, has been found on a specimen from the Kombat mine, Otavi Valley, Namibia. It is named yangite to honor the contributions of Hexiong Yang, Department of Geosciences, University of Arizona, to the fields of chain silicates in particular and mineralogy in general, and his stewardship of the RRUFF project's (http://rruff.info) ambitious attempt to characterize the known minerals chemically, structurally, and spectrographically. The new mineral and its name have been approved by the Commission on New Minerals and Nomenclature and Classification (CNMNC) of the International Mineralogical Association (IMA2012-052). Part of the co-type sample has been deposited at the University of Arizona Mineral Museum (Catalog no. 19341), the RRUFF Project (deposition no. R090031), and the Smithsonian Institution, Washington, D.C., U.S.A. (catalog number 175983). This paper describes the physical and chemical properties of yangite, and its single-crystal X-ray diffraction and Raman spectroscopic data.

* E-mail: rmthomps@email.arizona.edu

SAMPLE DESCRIPTION AND EXPERIMENTAL METHODS

Occurrence, physical, and chemical properties, and Raman spectra

Yangite was found on a single specimen from the Kombat mine, Namibia, in the collection of the late John Innes (Fig. 1). Innes was a senior mineralogist in the employ of the Tsumeb Corporation and has been honored for his studies of the geology and mineralogy of the Tsumeb and Kombat mines with a mineral name, johninnesite (cf. Innes and Chaplin 1986). He gave the piece to co-author Bill Pinch with the recognition that it was unique.

A brief summary of relevant geological information follows, taken from a detailed presentation of the geology of the Kombat Mine authored by Innes and Chaplin (1986). The Kombat mine, located in the Otavi Valley, 37 km east of Otavi and 49 km south of Tsumeb, is in a sequence of weakly metamorphosed, thin to massive bedded, shallow-water dolostones of the Upper Proterozoic Hüttenberg Formation. Six discrete bodies of brecciated, hydrothermally deposited massive sulfide ores are present along a disconformity separating dolostone from younger slate. Elements that occur in economic concentrations include copper, lead, and silver. Iron and manganese are abundant. Other elements found at Kombat in significant concentrations include zinc, barium, arsenic, chromium, molybdenum, chlorine, and germanium.

Yangite occurs in an epithermal association, one of seven described ore types. The others are massive and semi-massive sulfides, mineralized net-vein fracture systems, galena-rich alteration breccias, a pyrite-sericite association, an iron-manganese oxide/silicate association, and mineralized fracture fillings. The epithermal association postdates main mineralization and consists of vuggy veins

0003-004X/16/0011–2539$05.00/DOI: http://dx.doi.org/10.2138/am-2016-5682

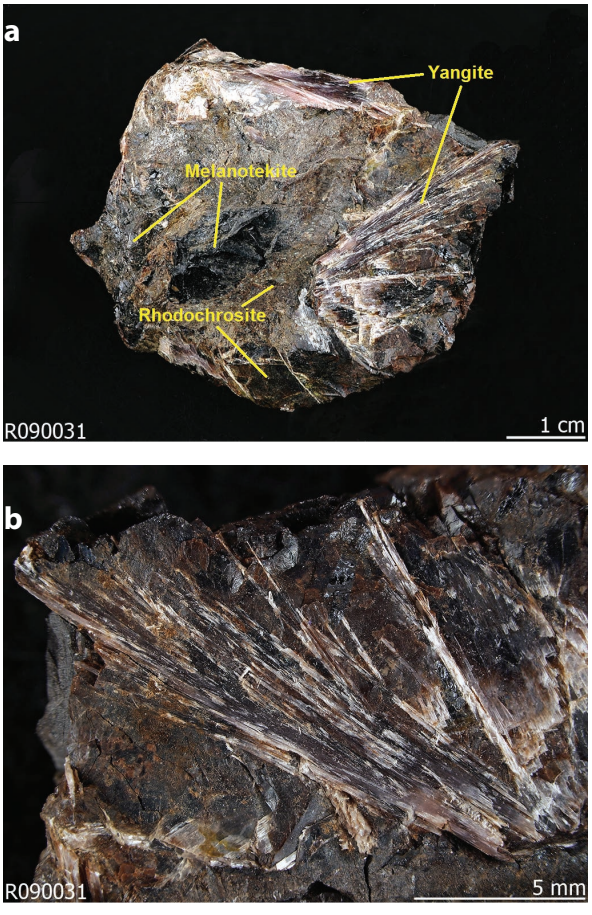

FIGURE 1. (**a**) Rock samples on which yangite crystals are found; (**b**) A microscopic view of yangite, associated with dark brown melanotekite. (Color online.)

of calcite, quartz, and chalcopyrite; narrow veins of galena, rhodochrosite, helvite, and barite; and a rare assemblage in the Kombat Central ore body of manganite-nambulite-serandite-barite-cahnite-brushite-kentrolite-calcite-gypsum. Yangite presumably comes from the narrow rhodochrosite-bearing veins.

Dunn (1991) reviewed rare minerals found in the Kombat Mine, including four Pb-silicates: barysilite, melanotekite, kentrolite, and molybdophyllite. Yangite increases the total of Pb-silicates to five, and is found in a massive assemblage with melanotekite $Pb_2Fe^{3+}_2O_2Si_2O_7$ and rhodochrosite $MnCO_3$. Figure 1 is a photograph of a spray of yangite in a matrix of black massive melanotekite and brown rhodochrosite. Broken pieces of yangite crystals are bladed or platy, elongated along [010], and up to 12 mm long. No twinning is apparent in any of the samples.

The mineral is colorless to pale brown in transmitted light under miscrscopy, transparent with white streak and vitreous luster. It is sectile and has a Mohs hardness of ~5; cleavage is perfect on {101} and no parting was observed. Fractures are uneven. The measured (by heavy-liquid) and calculated densities are 4.14(3) and 4.16 g/cm^3, respectively. Optically, yangite is biaxial (–), with $n_\alpha = 1.690(1)$, $n_\beta = 1.699(1)$, $n_\gamma = 1.705(1)$, $Y = b$, $Z \wedge c = 10.7°$, $2V_{meas} = 77(2)°$, and $2V_{calc} = 78°$. It is insoluble in water, acetone, and hydrochloric acid.

The chemical composition of yangite was determined with a CAMECA SX100 electron microprobe at 15 kV and 5 nA with a beam diameter of 20 μm. The standards include diopside for Si, rhodonite for Mn, and NBS_K0229 (Pb-glass) for Pb, yielding an average composition (wt%) (10 points) of SiO_2 36.59(19), MnO 14.45(11), PbO 45.46(41), H_2O 3.66 added on the basis of structural results, resulting in a total of 100.16(34). The presence of H_2O in yangite was confirmed by Raman spectroscopic measurements and structure determination (see below). Trace amounts of Fe and Ca were observed from WDS, but they were under the detection limits of the analysis. The resultant chemical formula, calculated on the basis of 9 O atoms (from the structure determination), is $Pb_{1.00}Mn_{1.00}Si_{3.00}O_8 \cdot H_2O$, or simply $PbMnSi_3O_8 \cdot H_2O$.

The Raman spectrum of yangite was collected from a randomly oriented crystal on a Thermo-Almega microRaman system, using a 532 nm solid-state laser with a thermoelectric cooled CCD detector. The laser is partially polarized with 4 cm^{-1} resolution and a spot size of 1 μm.

X-ray crystallography

Both powder and single-crystal X-ray diffraction data of yangite were collected on a Bruker X8 APEX2 CCD X-ray diffractometer equipped with graphite-monochromatized Mo$K\alpha$ radiation. However, it is difficult to unambiguously index all powder X-ray diffraction peaks due to severe peak overlaps. Table 1 lists the measured powder X-ray diffraction data, along with those calculated from the determined structure using the program XPOW (Downs et al. 1993).

Single-crystal X-ray diffraction data for yangite were collected from an untwinned, elongated tabular crystal (0.06 × 0.04 × 0.03 mm) with frame widths of 0.5° in ω and 30 s counting time per frame. All reflections were indexed on the basis of a triclinic unit cell (Table 2). No satellite or super-lattice reflections were observed. The intensity data were corrected for X-ray absorption using the Bruker program SADABS. The absence of any systematic absences of reflections suggest possible space groups $P1$ or $P\bar{1}$. The crystal structure was solved and refined using SHELX97 (Sheldrick 2008) based on the space group $P\bar{1}$ because it produced the better refinement statistics in terms of bond lengths and angles, atomic displacement parameters, and R factors. The positions of all atoms were refined with anisotropic displacement parameters, except for H atoms, which were

TABLE 1. Powder X-ray diffraction data for yangite

I_{meas}	d_{meas}	I_{calc}	d_{calc}	h	k	l
60	7.361	100.00	7.3796	$\bar{1}$	0	1
21	7.023	29.36	7.0353	0	0	1
31	6.671	46.90	6.6489	0	$\bar{1}$	1
30	6.000	31.96	5.9844	1	0	0
10	4.712	13.60	4.7204	$\bar{1}$	1	1
37	4.472	26.68	4.4677	1	$\bar{1}$	1
13	4.272	16.11	4.2765	$\bar{1}$	$\bar{1}$	2
14	3.806	18.74	3.8159	$\bar{2}$	1	1
42	3.697	42.50	3.7173	$\bar{2}$	0	1
		19.73	3.6898	$\bar{2}$	0	2
25	3.591	26.16	3.6054	0	1	1
35	3.514	35.74	3.5177	0	0	2
		9.66	3.5170	$\bar{2}$	1	0
10	3.409	15.52	3.4141	$\bar{1}$	$\bar{2}$	0
8	3.321	13.80	3.3244	0	$\bar{2}$	2
18	3.175	24.17	3.1817	$\bar{1}$	$\bar{1}$	3
12	3.111	16.02	3.1177	$\bar{1}$	1	2
53	2.985	35.99	2.9922	2	0	0
100	2.909	60.50	2.9171	1	$\bar{2}$	2
		51.74	2.9076	0	$\bar{2}$	0
		27.16	2.8953	$\bar{1}$	$\bar{2}$	2
17	2.761	12.30	2.7678	$\bar{1}$	$\bar{2}$	1
15	2.718	7.51	2.7196	$\bar{2}$	$\bar{1}$	1
23	2.447	18.77	2.4378	1	0	2
12	2.390	16.43	2.4003	$\bar{3}$	$\bar{2}$	1
6	2.332	4.36	2.3358	$\bar{1}$	$\bar{1}$	4
19	2.275	4.81	2.2775	0	$\bar{2}$	1
		5.80	2.2728	$\bar{1}$	$\bar{2}$	4
18	2.220	11.02	2.2338	2	$\bar{2}$	2
18	2.205	13.29	2.1999	1	$\bar{2}$	0
9	2.134	8.76	2.1469	1	$\bar{1}$	3
		5.28	2.1348	$\bar{3}$	$\bar{1}$	2
6	2.097	9.08	2.0898	$\bar{3}$	$\bar{1}$	4
9	2.077	4.75	2.0756	$\bar{1}$	0	4
7	2.064	6.60	2.0724	$\bar{1}$	$\bar{3}$	3
4	2.016	11.23	2.0264	$\bar{3}$	$\bar{2}$	1
8	1.931	9.46	1.9418	$\bar{3}$	2	3
4	1.856	3.94	1.8478	0	1	3
14	1.805	3.49	1.8027	0	2	2
22	1.783	6.68	1.7939	$\bar{3}$	$\bar{3}$	2
		5.28	1.7935	1	$\bar{2}$	4
		4.07	1.7915	2	0	2
10	1.704	5.57	1.7172	$\bar{3}$	$\bar{2}$	2
		4.22	1.7118	$\bar{1}$	2	3
15	1.673	7.83	1.6884	2	2	0
13	1.666	4.19	1.6648	3	0	1

not located from the difference Fourier maps. Final coordinates and displacement parameters of the atoms in yangite are listed in Table 3 and selected bond distances in Table 4. A CIF[1] is available.

DISCUSSION

Crystal structure

The crystal structure of yangite consists of double wollastonite SiO_4 tetrahedral chains running parallel to **b** and sharing corners with ribbons of Mn- and Pb-polyhedra (Fig. 2a). These double chains are characterized by alternating 4- and 6-membered tetrahedral rings, like those found in okenite, $Ca_{10}Si_{18}O_{46}\cdot 18H_2O$ (Fig. 2b) (Merlino 1983). In okenite, however, layers of parallel double chains stacked along c* alternate with sheets of tetrahedra composed of 5- and 8-membered rings. Similar double wollastonite chains have also been found in synthetic compounds (Haile and Wuensch 1997, 2000; Radić and Kahlenberg 2001; Radić et al. 2003).

There are three distinct tetrahedral Si sites in yangite, Si1, Si2, and Si3, with average Si-O bond distances of 1.622, 1.622, and 1.624 Å, respectively. Among them, the Si3 tetrahedron is the most distorted and the Si2 the least, as measured by tetrahedral angle variance and quadratic elongation (Robinson et al. 1971) (Table 4), but none are unusually distorted.

The Mn^{2+} cation is octahedrally coordinated. Bond-valence sums calculated using the parameters given by Brese and O'Keeffe (1991) indicate that Mn is 2+, rather than 3+, and that O9W is H_2O (Table 5). The cation coordination octahedron is relatively undistorted, especially given that one corner is anchored by a water molecule, with an angle variance of 34.06 and a quadratic elongation of 1.01.

The bonding topology of yangite was calculated using the procrystal representation of its electron density. Procrystal electron density is computed by summing the contributions of the spherically averaged electron density of neutral atoms placed at the experimentally determined locations of the atoms in a crystal (cf. Downs et al. 2002, Downs 2003 for details of the method and evidence of its accuracy and efficacy). Calculations

[1]Deposit item AM-16-115682, CIF. Deposit items are free to all readers and found on the MSA web site, via the specific issue's Table of Contents (go to http://www.minsocam.org/msa/ammin/toc/2016/Nov2016_data/Nov2016_data.html).

TABLE 2. Crystallographic data and refinement results for yangite

	Yangite	Hypothetical material
Ideal chemical formula	$PbMnSi_3O_8\cdot 2H_2O$	$Ca_2Si_3O_8\cdot 2H_2O$
Crystal symmetry	Triclinic	Triclinic
Space group	$P\bar{1}$ (#2)	$P\bar{1}$ (#2)
a (Å)	9.6015(9)	9.69
b (Å)	7.2712(7)	7.28
c (Å)	7.9833(8)	8.11
α (°)	105.910(4)	103.0
β (°)	118.229(4)	118.5
γ (°)	109.935(5)	112.1
V (Å^3)	392.69(7)	404.30
Z	2	2
ρ_{cal} (g/cm^3)	4.164	
λ (Å, Mo*K*α)	0.71073	
μ (mm^{-1})	23.501	
2θ range for data collection	≤65.58	
No. of reflections collected	9930	
No. of independent reflections	2848	
No. of reflections with $I > 2\sigma(I)$	2460	
No. of parameters refined	128	
R(int)	0.042	
Final R_1, wR_2 factors [$I > 2\sigma(I)$]	0.031, 0.063	
Final R_1, wR_2 factors (all data)	0.040, 0.066	
Goodness-of-fit	1.00	
Reference	This work	Merlino and Bonaccorsi (2008)

TABLE 4. Selected bond distances (Å) in yangite

Si1-O1	1.599(3)	Si2-O3	1.624(3)	Si3-O2	1.650(3)
Si1-O2	1.626(4)	Si2-O4	1.630(4)	Si3-O5	1.655(3)
Si1-O3	1.635(3)	Si2-O5	1.619(3)	Si3-O7	1.594(4)
Si1-O4	1.629(3)	Si2-O6	1.613(4)	Si3-O8	1.599(4)
Avg.	1.622		1.622		1.624
TAV	13.73		11.24		20.95
TQE	1.0031		1.0027		1.0049
Pb-O1	2.684(3)	Mn-O1	2.200(3)		
Pb-O6	2.333(3)	Mn-O1	2.245(3)		
Pb-O6	2.770(3)	Mn-O6	2.300(3)		
Pb-O7	2.412(3)	Mn-O7	2.124(3)		
Pb-O8	2.397(3)	Mn-O8	2.138(3)		
Pb-O5	3.063(3)	Mn-O9w	2.188(4)		
Avg.	2.610	Avg.	2.199		
		OAV	34.06		
		OQE	1.0104		

Note: TAV = tetrahedral angle variance; TQE = tetrahedral quadratic elongation OAV = octahedral angle variance; OQE = octahedral quadratic elongation (Robinson et al. 1971).

TABLE 5. Calculated bond-valence sums for yangite

	O1	O2	O3	O4	O5	O6	O7	O8	O9w	Sum
Pb	0.21			0.02	0.03	0.55	0.44	0.46	0.01	1.95
					0.06	0.17				
Mn	0.33					0.25	0.40	0.39	0.35	2.01
	0.29									
Si1	1.07	1.00	0.98	0.99						4.04
Si2			0.99	0.98	1.01	1.03				4.01
Si3		0.93			0.92		1.09	1.07		4.01
Sum	1.90	1.93	1.97	1.99	2.02	2.00	1.93	1.92	0.36	

Note: The parameters used for the calculations were from Brese and O'Keeffe (1991).

TABLE 3. Atomic coordinates and displacement parameters for yangite

Atom	*x*	*y*	*z*	U_{iso}	U_{11}	U_{22}	U_{33}	U_{23}	U_{13}	U_{12}
Pb	0.22536(3)	0.73792(3)	0.05494(3)	0.0132(1)	0.0134(1)	0.0145(1)	0.0143(1)	0.0075(1)	0.0098(1)	0.0084(1)
Mn	0.1787(1)	0.2238(1)	0.0739(1)	0.0102(1)	0.0091(3)	0.0102(3)	0.0112(3)	0.0056(3)	0.0060(3)	0.0057(3)
Si1	0.1178(2)	0.2686(2)	0.4471(2)	0.0080(2)	0.0078(6)	0.0080(6)	0.0084(6)	0.0046(5)	0.0049(5)	0.0046(5)
Si2	0.1430(2)	0.8580(2)	0.4314(2)	0.0086(2)	0.0089(6)	0.0096(6)	0.0098(6)	0.0058(5)	0.0062(5)	0.0063(5)
Si3	0.4104(2)	0.7099(2)	0.5425(2)	0.0087(2)	0.0061(6)	0.0075(6)	0.0095(6)	0.0041(5)	0.0035(5)	0.0037(5)
O1	0.0058(5)	0.1535(6)	0.1840(6)	0.0107(6)	0.010(2)	0.013(2)	0.009(2)	0.006(1)	0.005(1)	0.006(1)
O2	0.3099(5)	0.5233(6)	0.5936(6)	0.0105(6)	0.009(2)	0.007(2)	0.010(2)	0.004(1)	0.004(1)	0.002(1)
O3	0.1868(5)	0.1149(6)	0.5347(6)	0.0101(6)	0.012(2)	0.010(2)	0.011(2)	0.007(1)	0.007(1)	0.008(1)
O4	–0.0103(5)	0.2891(6)	0.5213(6)	0.0135(7)	0.017(2)	0.013(2)	0.021(2)	0.012(1)	0.015(2)	0.011(1)
O5	0.3482(5)	0.8942(6)	0.5801(6)	0.0122(7)	0.011(2)	0.011(2)	0.014(2)	0.006(1)	0.006(1)	0.009(1)
O6	0.0403(5)	0.7286(6)	0.1679(6)	0.0112(7)	0.012(2)	0.013(2)	0.009(2)	0.006(1)	0.007(1)	0.007(1)
O7	0.3252(5)	0.5838(6)	0.2877(6)	0.0129(7)	0.015(2)	0.012(2)	0.012(2)	0.006(1)	0.008(1)	0.008(1)
O8	0.6363(5)	0.8585(6)	0.7301(6)	0.0110(7)	0.008(2)	0.011(2)	0.015(2)	0.007(1)	0.006(1)	0.005(1)
O9W	0.3552(6)	0.3169(9)	0.9730(7)	0.033(1)	0.016(2)	0.051(3)	0.018(2)	0.013(2)	0.011(2)	0.009(2)

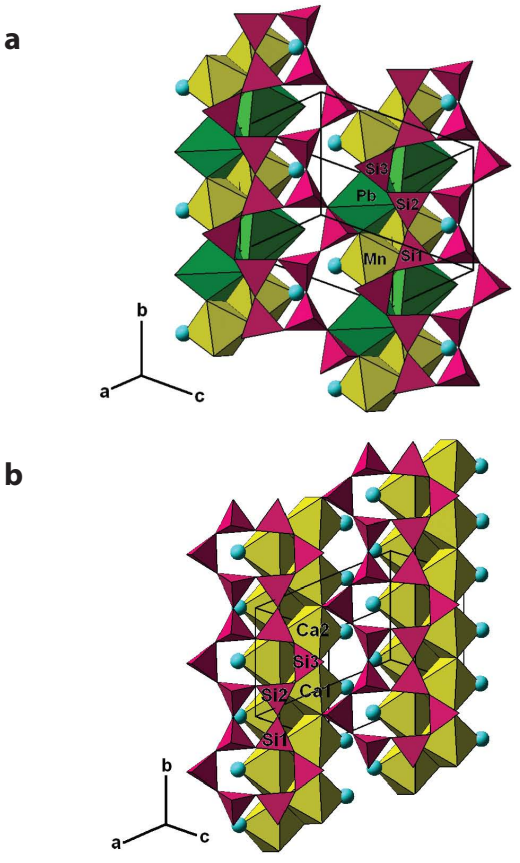

FIGURE 2. (**a**) Crystal structure of yangite, showing the double chains of SiO_4 tetrahedra and ribbons of Mn- and Pb-polyhedra. (**b**) A portion of the okenite structure (Merlino 1983), showing its similarity to the yangite structure. The spheres in both figures represent H_2O. (Color online.)

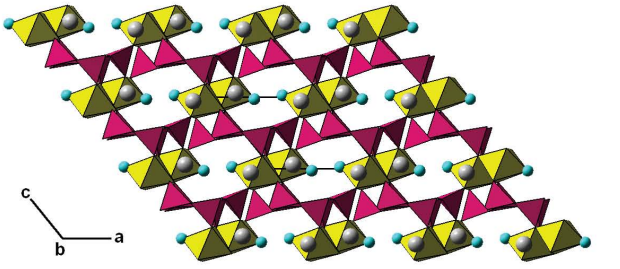

FIGURE 3. Crystal structure of yangite. The large and small spheres represent Pb and H_2O groups, respectively. The octahedra and tetrahedra represent MnO_6 and SiO_4 groups, respectively. For clarity, no chemical bonds are drawn for Pb. (Color online.)

were performed with in-house software using the most accurate available analytical Hartree-Fock wave functions (Koga et al. 1999, 2000; Thakkar and Koga 2003).

The results suggest that Pb^{2+} is fivefold-coordinated, with all Pb-O bond distances shorter than 2.770 Å (Table 4). As explained in the companion paper (Thompson et al. this issue), geometrical constraints in pyroxenoids arising from the nature of the octahedral and tetrahedral chains dictate that at least one *M* site must be very distorted.

Procrystal calculations also indicate the presence of a three weak O9W-O bonds and a weak, long O9W-Pb interaction that bridges the channel between the parallel bands of Mn/Pb polyhedra. Interestingly, the computation was performed using an oxygen atom at the location of O9W, i.e., without the protons. It is not possible to determine the nature of these bonds given that the unlocated hydrogen atoms were disregarded in the computation, but it is certainly possible that the Pb^{2+} lone pair is involved in a hydrogen bond with O9W. However, it is not obvious how the hydrogens fit into the structure. A more extensive discussion of this issue is in the companion paper (Thompson et al. this issue).

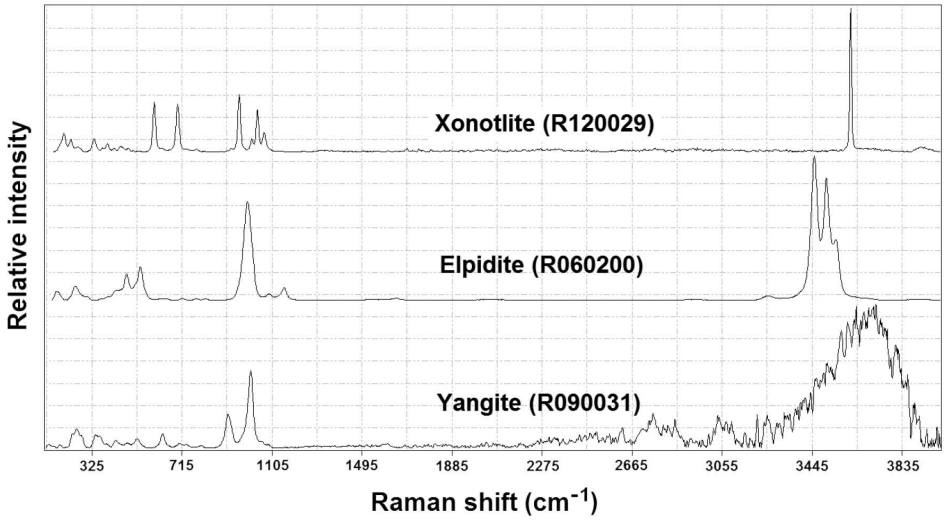

FIGURE 4. Raman spectrum of yangite, along with the Raman spectra of xonoltite and elpidite for comparison. The spectra are shown with vertical offset for more clarity.

The bulk structure of yangite can be regarded as layers of SiO_4 tetrahedra alternating with those of Mn- and Pb-polyhedra stacked along **c*** (Fig. 3). For an analysis of the structural relationships between yangite and other pyroxenoids, see the companion paper, Thompson et al. (this issue).

Raman spectra

There have been numerous Raman spectroscopic studies on materials with wollastonite-like silicate chains (e.g., Mills et al. 2005; Makreski et al. 2006; Wierzbicka-Wieczorek et al. 2010; Can et al. 2011). In particular, Frost et al. (2012) measured the Raman spectra of xonotlite, a mineral with one-connected double wollastonite chains (the *n-connected* terminology describes the number of connecting tetrahedra between chains and is due to Merlino and Bonaccorsi 2008). The Raman spectrum of yangite is displayed in Figure 4, along with the Raman spectra of xonotlite and elpidite taken from the RRUFF Project (R120029 and R060200, respectively) for comparison.

Due to extremely strong sample fluorescence, we were unable to improve the spectral quality of yangite above 1500 cm^{-1}. Nonetheless, the broad bands between 3200 and 3850 cm^{-1} may be ascribed to the O-H stretching vibrations. The two sharp bands at 1015 and 916 cm^{-1} are due to the Si-O stretching vibrations within the SiO_4 groups, whereas the bands between 300 and 900 cm^{-1} are primarily attributable to the O-Si-O and Si-O-Si angle bending vibrations (Dowty 1987; Makreski et al. 2006; Frost et al. 2012). The bands below 320 cm^{-1} are of a complex origin, mostly associated with the rotational and translational modes of SiO_4 tetrahedra, Mn-O and Pb-O interactions.

Implications

A great number of natural and synthetic phases, mostly hydrous Ca-silicates, display crystal structures characterized by the presence of double wollastonite chains. Merlino and Bonaccorsi (2008) presented a thorough review of such compounds and classified them into three categories based on the number of tetrahedra shared between two single chains: one-, two-, and three-connected chains, exemplified by those in xonotlite, okenite, and elpidite, respectively. However, unlike xonotlite or elpidite, okenite is not a "pure" chain silicate, as its structure consists of both silicate chains and sheets (Merlino 1983). Therefore, yangite represents the first chain silicate with two-connected double chains. Furthermore, the discovery of yangite implies that more Pb-silicate compounds or minerals with the chemical formula $PbMSi_3O_8 \cdot H_2O$ (M = Fe^{2+}, Ca^{2+}, Mg^{2+}, and other divalent cations) may be synthesized or found in nature, as substitution between Mn and other divalent cations is common in pyroxenoids.

By eliminating the silicate tetrahedral sheets in the okenite structure, Merlino and Bonaccorsi (2008) derived a hypothetical structure with the composition $Ca_2Si_3O_8 \cdot 2H_2O$, space group $P\bar{1}$, and unit-cell parameters $a = 9.69$, $b = 7.28$, $c = 8.11$ Å, $\alpha = 103.0$, $\beta = 118.5$, $\gamma = 112.1°$ (Table 2). Most remarkably, comparison of yangite and the model structure proposed by Merlino and Bonaccorsi (2008) reveals that, except for the amount of H_2O, this hypothetical phase possesses all of the structural features found in yangite (Table 2, Fig. 2). The differences in the H_2O contents and unit-cell parameters between the hypothetical phase and yangite are most likely to result from the substitution of larger Pb^{2+} with its lone-pair electrons for smaller Ca^{2+}.

Acknowledgments

This study was funded by Science Foundation Arizona. We are grateful to Stefano Merlino for providing us with his unpublished data and Ajit Thakkar for providing us with his electron wave functions. We also thank Merlino and two anonymous reviewers, along with Associate Editor Fernando Colombo, for their comments, which have improved the quality of this manuscript.

References cited

Brese, N.E., and O'Keeffe, M. (1991) Bond-valence parameters for solids. Acta Crystallographica, B47, 192–197.

Can, N., Guinea, J.J.G., Kibar, R., and Cetin, A. (2011) Luminescence and Raman characterization of rhodonite from Turkey. Spectroscopy Letters, 44, 566–569.

Downs, R.T. (2003) Topology of the pyroxenes as a function of temperature, pressure, and composition as determined from the procrystal electron density. American Mineralogist, 88, 556–566.

Downs, R.T., Bartelmehs, K.L., Gibbs, G.V., and Boisen, M.B. Jr. (1993) Interactive software for calculating and displaying X-ray or neutron powder diffractometer patterns of crystalline materials. American Mineralogist, 78, 1104–1107.

Downs, R.T., Gibbs, G.V., Boisen, M.B. Jr., and Rosso, K.M. (2002) A comparison of procrystal and ab initio representations of the electron-density distributions of minerals. Physics and Chemistry of Minerals, 29, 369–385.

Dowty, E. (1987) Vibrational interactions of tetrahedra in silicates glass and crystals: II. Calculations on melilites, pyroxenes, silica polymorphs and feldspars. Physics and Chemistry of Minerals, 14, 122–138.

Dunn, P.J. (1991) Rare minerals of the Kombat Mine. Mineralogical Record, 22, 421–424.

Frost, R.L., Mahendran, M., Poologanathan, K., and Xi, F. (2012) Raman spectroscopic study of the mineral xonotlite $Ca_6Si_6O_{17}(OH)_2$—A component of plaster boards. Materials Research Bulletin, 47, 3644–3649.

Haile, S.M., and Wuensch, B.J. (1997) Comparison of the crystal chemistry of selected MSi_6O_{15}-based silicates. American Mineralogist, 82, 1141–1149.

——— (2000) Structure, phase transitions and ionic conductivity of $K_3NdSi_6O_{15} \cdot xH_2O$. I. α-$K_3NdSi_6O_{15} \cdot 2H_2O$ and its polymorphs. Acta Crytallographica, B56, 335–345.

Innes, J., and Chaplin, R.C. (1986) Ore bodies of the Kombat Mine, South West Africa/Namibia. In C.R. Anhaeusser and S. Maske, Eds., Mineral Deposits of South Africa, vol. 1 and 2, p. 1789–1805. Geological Society of South Africa, Johannesburg, Republic of South Africa.

Koga, T., Kanayama, K., Watanabe, T., and Thakkar, A.J. (1999) Analytical Hartree-Fock wave functions subject to cusp and asymptotic constraints: He to Xe, Li^+ to Cs^+, H^- to I^-. International Journal of Quantum Chemistry, 71, 491–497.

Koga, T., Kanayama, K., Watanabe, T., Imai, T., and Thakkar, A.J. (2000) Analytical Hartree-Fock wave functions for the atoms Cs to Lr. Theoretical Chemistry Accounts, 104, 411–413.

Makreski, P., Jovanovski, G., Gajovic, A., Biljan, T., Angelovski, D., Jacimovic, R. (2006) Minerals from Macedonia. XVI. Vibrational spectra of some common appearing pyroxenes and pyroxenoids. Journal of Molecular Structure, 788, 102–114.

Merlino, S. (1983) Okenite, $Ca_{10}Si_{18}O_{46} \cdot 18H_2O$: the first example of a chain and sheet silicate. American Mineralogist, 68, 614–622.

Merlino, S., and Bonaccorsi, E. (2008) Double wollastonite chains: Topological/conformational varieties, polytypic forms, isotypic compounds. Zeitschrift für Kristallographie, 223, 85–97.

Mills, S.J., Ray L. Frost, R.L., Kloprogge, J.T., and Weier, M.L. (2005) Raman spectroscopy of the mineral rhodonite. Spectrochimica Acta, 62, 171–175.

Radić, S., and Kahlenberg, V. (2001) Single crystal structure investigation of twinned $NaKSi_2O_5$—a novel sinlge layer silicate. Solid State Sciences, 3, 659–667.

Radić, S., Kahlenberg, V., and Schmidt, B.C. (2003) High-pressure mixed alkli dislicates in the system $Na_{2-x}K_xSi_2O_5$: Hydrothermal synthesis and crystal structures of $NaKSi_2O_5$-II and $Na_{0.67}K_{1.33}Si_2O_5$. Zeitschrift für Kristallographie, 218, 413–420.

Robinson, K., Gibbs, G.V., and Ribbe, P.H. (1971) Quadratic elongation, a quantitative measure of distortion in coordination polyhedra. Science, 172, 567–570.

Sheldrick, G.M. (2008) A short history of *SHELX*. Acta Crystallographica, A64, 112–122.

Thakkar, A.J., and Koga, T. (2003) Analytic Hartree-Fock wave functions for atoms and ions. In E.J. Brändas and E.S. Kryachko, Eds., Fundamental World of Quantum Chemistry: A tribute to the memory of Per-Olov Löwdin, vol. I, p. 587–599. Kluwer, Dordrecht.

Thompson, R.T., Yang, H., and Downs, R.T. (2016) Ideal wollastonite and the relationship between the pyroxenoids and pyroxenes. American Mineralogist, 101, 2544–2553.

Wierzbicka-Wieczorek, M., Kolotsch, U., Nasdala, L., and Tillmanns, E. (2010) $K_{2.9}Rb_{0.1}ErSi_3O_9$: a novel, non-centrosymmetric chain silicate and its crystal structure. Mineralogical Magazine, 74, 979–990.

Manuscript received January 13, 2016
Manuscript accepted July 6, 2016
Manuscript handled by Fernando Colombo